Current Trends in Polymer Science

S. Koltzenburg et al., *Polymer Chemistry*, DOI 10.1007/978-3-662-49279-6_22

22

In this chapter some developments are discussed that have caught our attention over the past few years for a variety of reasons. The selection is, of course, subjective, and no attempt is made to suggest whether these developments are likely to become widespread technology or remain laboratory curiosities. Nevertheless, we believe the examples presented are interesting in their originality and show some of the directions being followed in current polymer science.

22.1 Nanocomposites

Nanocomposites consist of two or more types of organic or inorganic macromolecules that form structures in the dimension of nanometers, or are even molecularly mixed. Such materials are playing increasingly important roles as surface coatings, reinforcements, and barrier materials. Monolithic nanocomponents are interesting precursors for highly porous oxides and polymer networks. Because of their large internal surface, such materials have potential, for example, for gas storage.

There are various strategies for synthesizing nanocomposites, for example, *simultaneous polymerization* whereby two monomers A and B are polymerized side by side (simultaneously) (Fig. 22.1).

Furfuryl alcohol is polymerized cationically; the water produced induces the sol–gel process, in which $Si(OR)_4$ is converted into SiO_2. This process is by no means trivial; the phase separation during and after the synthesis can negatively influence the dimensions of the structural elements formed.

Consecutive polymerization is an alternative to simultaneous polymerization. As shown in Fig. 22.2, the functions A and B of a monomer are activated successively.

However, the most promising method is *twin polymerization*, which occurs as shown in Fig. 22.3 (Grund et al. 2007; Spange and Grund 2009).

If the polymerization of blocks A and B can be made to occur undisturbed side by side—without interruptions by phase separation or copolymerization—one can achieve products with a large internal surface area (800–1000 $m^2\ g^{-1}$) after removing one of the components.

Figure 22.4 gives a selection of A, B monomers that have been successfully used in twin polymerization.

The ionic polymerization of tetrafurfuryloxysilane results in a nanostructured network. It can be shown by ^{13}C and ^{29}Si-solid nuclear magnetic resonance, as well as by chemical analyses that form in the process two independent networks that are intertwined but not chemically connected with one another, called interpenetrating networks.

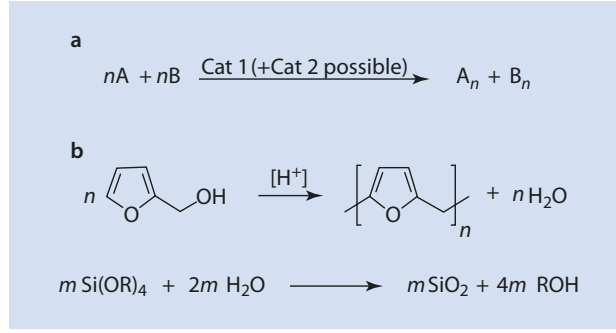

Fig. 22.1 Simultaneous polymerization. (**a**) Schematically. (**b**) Example: polymerization of furfuryl alcohol and tetraalkoxysilane

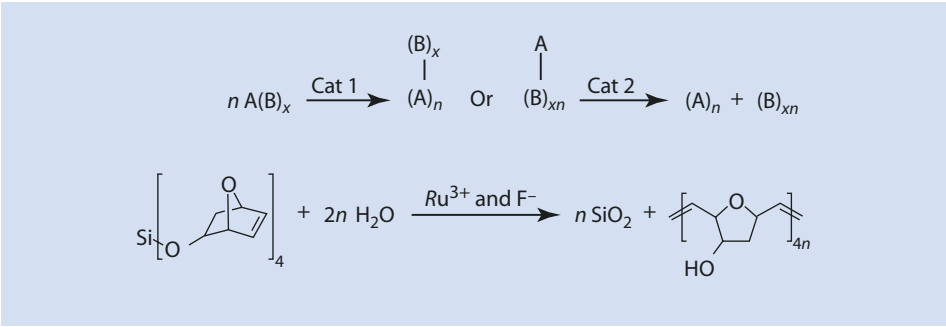

Fig. 22.2 Scheme of consecutive polymerization

Fig. 22.3 Scheme of a twin-polymerization

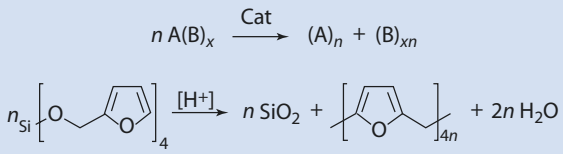

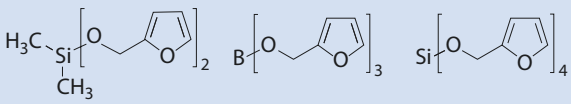

Fig. 22.4 Examples of bi-, tri-, and tetra-functional molecules that are suitable as monomers for twin-polymerization

After burning the organic phase of the nanocomposite of polyfurfuryl alcohol/SiO_2, one obtains monolithic SiO_2 particles with a surface area of 1000 $m^2\ g^{-1}$. If the inorganic polymer is selectively and successfully removed, one obtains an organic network. In the case of the nanocomposite composed of polyfurfuryl alcohol/SiO_2, however, this is impossible because the organic network is damaged by removing the SiO_2 (depolymerization).

The cationic polymerization of 2.2-spiro[4*H*-1,2,3-benzodioxasilane] has been shown to be more successful. The subsequent selective removal of the inorganic or the organic network results in stable carbon or SiO_2 monoliths with surface areas in the region of 1000 $m^2\ g^{-1}$.

The possible variations of the inorganic part of the A, B monomer is evident. The search for suitable organic ligands has proven more difficult. With the discovery of spiro molecules (Fig. 22.5), an interesting and promising way to produce materials with very small particle sizes in the range of 0.5–2 nm and extremely small and uniform pore diameters seems to have been found.

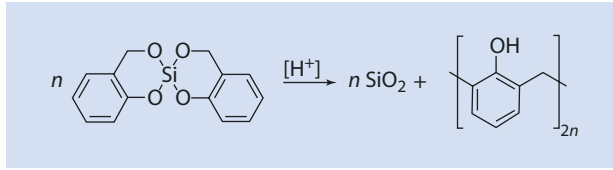

Fig. 22.5 Twin-polymerization of a spiro-A,B-monomer

22.2 Electrospinning: Facile Route to Nanofibers

Electrospinning is an easy and elegant method for producing very fine polymer fibers (Reneker and Chun 1996). In Fig. 22.6 an electrospinning apparatus is shown schematically. It consists of relatively few components; a syringe, a nozzle (usually a hollow needle), a high voltage power supply, and a collector.

First, the polymer solution to be spun is placed in a syringe out of which it is continuously pushed through a tight hollow needle (spinneret) as a thin stream. The syringe is depressed slowly and steadily, for example, by an electric motor with precision gearing.

To initiate the spinning process, an electrical field is generated between the metallic spinneret and the collector. The voltages of 1–30 kV are produced by a high voltage power supply.

When applied, the high voltage charges the drops conveyed from the spinneret, and the charge distributes itself equally on the surface of the polymer solution. Only two electrostatic forces have an effect on these drops—an electrostatic repulsion between the individual charges on the surface of the material exiting the spinneret and the Columbic attraction in the direction of the collector. A third force, the surface tension, opposes the electrostatic forces and initially inhibits movement of the drop induced by the other two forces. However, the initial, spherical drop is conically deformed by the effect of the electrostatic forces to form what is known as a Taylor cone. If the electrostatic forces are greater than the surface tension of the polymer solution, the solution is forced from the drop as a thin jet and is accelerated in the direction of the collector; velocities of several meters per second can develop. The solvent continuously evaporates, and the thread of polymer solution is stretched so that it arrives at the collector solution-free and with a drastically reduced diameter of the order of nanometers. There, over time, it forms a disorderly fiber mat. More modern techniques can produce an ordered, for example, parallel, deposition of fibers.

The morphology of the electrically spun fibers is defined by the intrinsic qualities of the polymer solution. The key parameters are summarized in Table 22.1.

The literature is inconsistent as to the effect of the various parameters given in Table 22.1. For example, although a decrease of the fiber diameter with increasing field strength has been widely discussed, the opposite has also been reported. Nevertheless, this technology has already been used successfully for many different polymers (Table 22.2).

The most important application of traditional fibers is the reinforcement of a large variety of materials. Nanofibers should interact much more successfully with the matrix than traditional fibers because of their high aspect ratio (length/diameter).

A further use for these fibers is as filter elements. With the filter mats made from nanofibers, particles with $d < 0.5$ µm can be filtered. In the field of air filtration, such systems are said to have great potential.

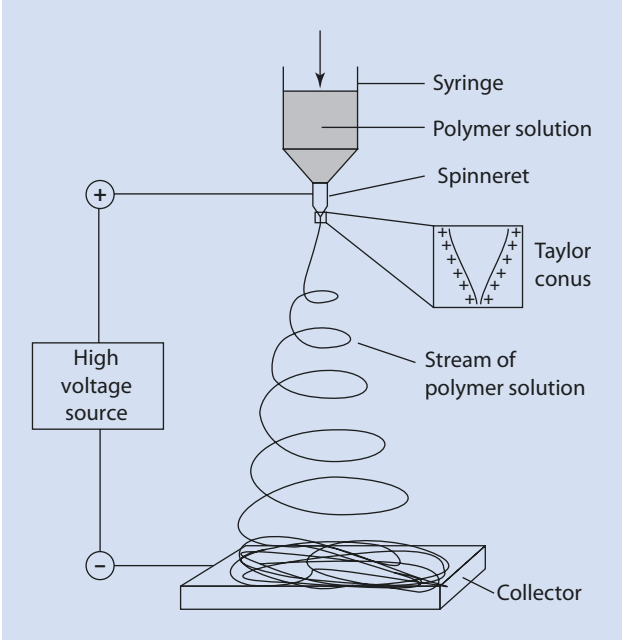

Fig. 22.6 Scheme for the electrospinning process

Table 22.1 Key parameters for the electrospinning process (Li and Xia 2004)

Intrinsic polymer solution parameter	Process parameter
Polymer type	Field strength
Conformation of the polymer chain	Distance between spinneret and collector
Viscosity or concentration of the polymer solution	Flow rate of the polymer solution Ambient humidity and temperature
Elasticity	
Electrical conductivity	
Polarity and surface tension of the solvent	

Because of their large specific surface area, nanofibers are ideal substrates for catalysts.

A broad and highly promising area of use of these fibers is in medicine, for example, as a support for soft tissue and blood vessels. They have also been proposed as a coating for hard prostheses. Moreover, their use as a support material for *tissue engineering*, the specified growth of cellular tissue on a carrier material, is also plausible because the similarity of these fibers to the native extracellular matrix encourages the colonization of cells.

A further application is in the treatment of wounds, in which fibers (possibly infused with medication) are spun directly onto the skin and can thus protect injured areas against viruses and bacteria.

Table 22.2 Electrospun polymers—selected examples

Polymer	Solvent	Possible application
Nylon 6,6	Formic acid	Safety clothes
Polyurethane	DMF	Safety clothes, filter elements
Polybenzimidazole	DMAc	Safety clothes
Polycarbonate	Dichloromethane	Sensors, filter elements
Polyacrylonitrile	DMF	Carbon fibers
Polylactide	Dichloromethane	Medical applications
Polyethylene oxide	Isopropanol/H_2O	Filter elements
Polystyrene	THF	Catalyst support, filter elements
Polyvinyl phenol	THF	Antimicrobial action
Cellulose acetate	Acetone	Membranes
Poly(2-hydroxyethyl-methacrylate)	Ethanol/formic acid	Flat tapes
Polyvinylidene fluoride	DMF/DMAc	Flat tapes

DMF Dimethyl formamide, *DMAc* Dimethyl acetamide

22.3 Spinning-Disc Reactor (SDR)

The success of a polymerization process depends not only on its kinetics but also on the way it is carried out. Polymerization in continuous or discontinuous processes in stirred tanks, stirred cascades, loop reactors, or flow tubes determines the morphology, molar mass, molar mass distribution, branching, or, if applicable, the cross-linking of the product and thus also determines the useful characteristics of the polymers produced. All reactor types can be traced back to three basic types (Fig. 22.7).

These three basic types—stirred tanks, continuously stirred tanks and flow reactors—are used in many variations and also combined with each other (Echte 1993). Nowadays such reactors are well understood. However, new challenges in the field of process control continue to arise. The term *process intensification* summarizes a response to the demands of modern process technology to reduce energy usage, required space, inventory of product and raw materials, number of process steps, emissions and noise and to increase efficiency and safety. The SDR (Fig. 22.8) is one solution to all of the above (Ramshaw 1983; Cai 2006; Pask et al. 2012).

In the SDR, a very thin liquid film is formed on a thermostatted rotating disc from a centrally added mixture of liquids or separated educts added at the center of the disc. The reaction mixture is tangentially accelerated by the shear stress acting at the interface between the disc and the liquid. The desired reaction occurs on the thermostatted disc. The product is spun onto the cooled outer wall, and collected at an outlet. The continuous operation, short retention time, and excellent heat transfer and mixing render this reactor of interest for polymerization reactions as long as the viscosity of the resulting product solution is not too high. It has been shown, for example, that from polyols and diisocyanates, polyurethane-pre-polymers of varying compositions and molar mass can be produced.

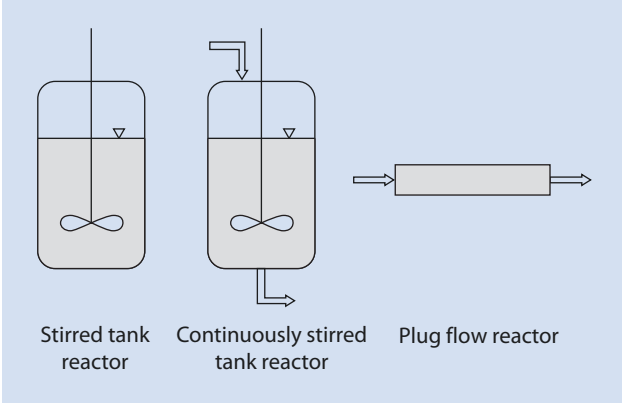

Fig. 22.7 Basic types of chemical reactors

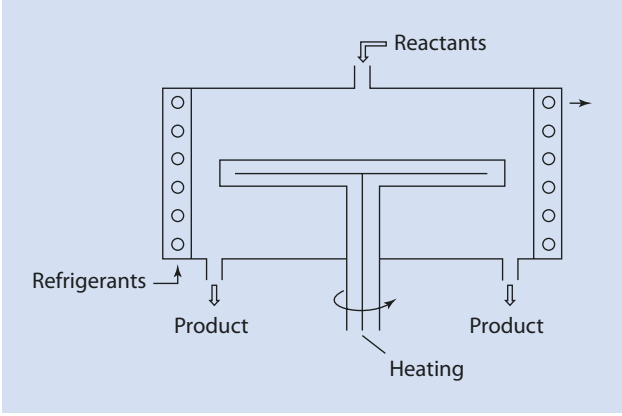

Fig. 22.8 Sketch of a spinning-disc reactor (SDR)

Polyreactions can be optimized in a short time and with comparatively small amounts of material by optimizing the disc temperature, the speed of the disc's rotation, and the flow rate. This reactor is also very suitable for photopolymerizations because light can easily and completely penetrate the ultrathin coating (from nanometers to micrometers, depending on the viscosity) on the rotating disc.

The advantages of the SDR compared to the stirred tank reactor are summarized in Table 22.3. In order to produce 3.6 tons of product requires 16 h in the stirred tank but in an SDR with a disc diameter of 1 m only 10 h.

In the SDR, the amount of substance per unit time is very small so that, in the event of an incident, only milliliters have to be discarded as compared to the total batch in the stirrer tank. Further advantages are its flexibility, for example, product change, but also the small amount of cleaning materials required, the relatively low investment costs, and the small size of the reactor.

In terms of process engineering, the SDR is particularly advantageous, compared to the discontinuous stirred tank reactor, when scaling-up a reaction (turning a laboratory experiment into an industrial process) because with the SDR this can be done without the use of characteristic numbers such as Reynolds-Prantl number and others (Table 22.4).

The tenfold multiplication of the diameter requires only one action: increasing the flow by a factor of 100. Thus, the film thickness and residence time remain identical. In a stirred tank reactor the transition from laboratory to the ton scale is much more laborious

Table 22.3 Comparison between an SDR and a stirred tank reactor using the example of the synthesis of polyurethane prepolymers (Cai 2006)

Reactor type	Stirred tank	SDR
Size	4 m^3—volume	100 cm—disc diameter
Charging	1.5 h	100 mL s^{-1}
Heating	2.5 h	27 min
Reaction	7 h	3 s
Cooling	1.5 h	20 min
Emptying	1.5 h	100 mL s^{-1}
Cleaning	2 h	100 mL s^{-1}
Total time	**16 h**	**10 h**
Production volume	**3600 kg**	**3600 kg**
Cleaning material	1000 kg	12.5 kg

Table 22.4 Parameters for the scale-up of an SDR process

Disc diameter (m)	Flow rate (mL s^{-1})	Film thickness (µm)	Residence time (s)	Production (t/8000 h)[a]
0.1	2	68.9	0.27	58
0.3	18	68.9	0.27	518
1.0	200	68.9	0.27	2880

[a]Assumption: annual available production time = 8000 h

and requires attention to, for example, the decrease of surface area to volume (which leads to different cooling characteristics) and the increase in the size of the stirrer (which leads to different shear and mixing parameters), to name just a few of the challenges.

22.4 Polymers for Organic Light-Emitting Diodes (OLEDs)

With the discovery that some organic substances display electroluminescence when voltages of less than 10 V are applied to them (Tang and van Slyke 1987) and that certain polymers also display this characteristic (Friend et al. 1999), a rapid development started, resulting in the multicolored light-emitting diodes that now cover the entire visible spectrum (Müller et al. 2003). The structure of a multilayer light-emitting diode is shown in Fig. 22.9.

The organic material (polymer or small molecule) is present in one or more layers of varying composition between a cathode and an anode on a glass substrate. Electrons flow into the organic phase at the cathode (Ba, Ca, or Al) and migrate through the electron conducting layer (I) to reach the emitter layer (II). There they encounter electron holes, which are formed

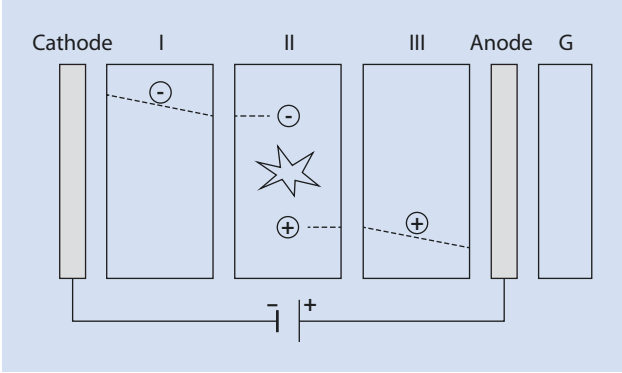

Fig. 22.9 Schematic construction of a three-layer OLED. *I* Electron Conductor, *II* Emitter, *III* Hole conductor, *G* Glass support, *Cathode* Ba, Ca, Al, *Anode* ITO (indium tin oxide)

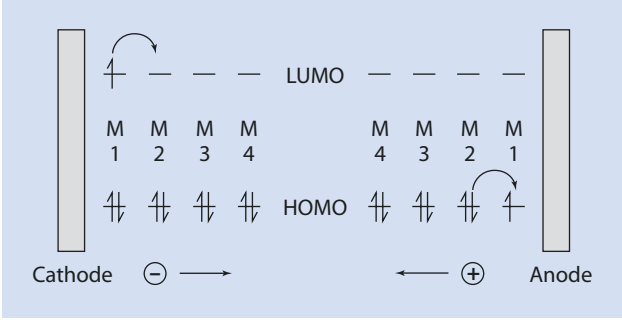

Fig. 22.10 Schematic representation of the electron and hole conduction through the organic layers of an OLED

at the anode by electrons being removed from the hole conducting layer (III). During the collision, they form an excited singlet state which relaxes to the ground state, emitting light. The emitted light passes through the transparent indium tin oxide (ITO) anode and then through the glass surface layer. The passage of the electrons and holes is outlined in Fig. 22.10.

The electron conduction occurs in the lowest unoccupied molecular orbit (LUMO). Without mass transport, the electron jumps from molecule to molecule toward the anode. Hole conduction occurs in the highest occupied molecular orbit (HOMO). The hole which is formed by "sucking up" an electron at the anode (electron deficient) is filled under the influence of the electrical field of its neighbor, leading to a hole there. From a chemical perspective, electron and hole conduction are a sequence of redox reactions driven by the electrical field. The reactions take place via radical cations (holes) and radical anions. The negative charge travels, without mass transport, from left to right and the positive charge in the opposite direction. Typical examples of electron and hole conductors are given in Fig. 22.11.

The basic processes for producing OLEDs are sublimation (*vapor deposition*) and preparation from solution (e.g., by so-called *spin coating*, whereby a coating is formed on a rotating surface by distributing the solution over the surface by centrifugal force). Sublimation technology is expensive and unsuitable for polymers. For smaller, high-performance OLEDs, sublimation is the method of choice because of the additional cleaning step involved in spin coating and the possibility of generating multilayered OLEDs without damaging the previously applied layer.

Polymers are applied exclusively from solution. Therefore the application of second and third polymer layers in the multilayered construction presents a challenge during the application process, as previously formed layers can redissolve. The problem can be simply solved by

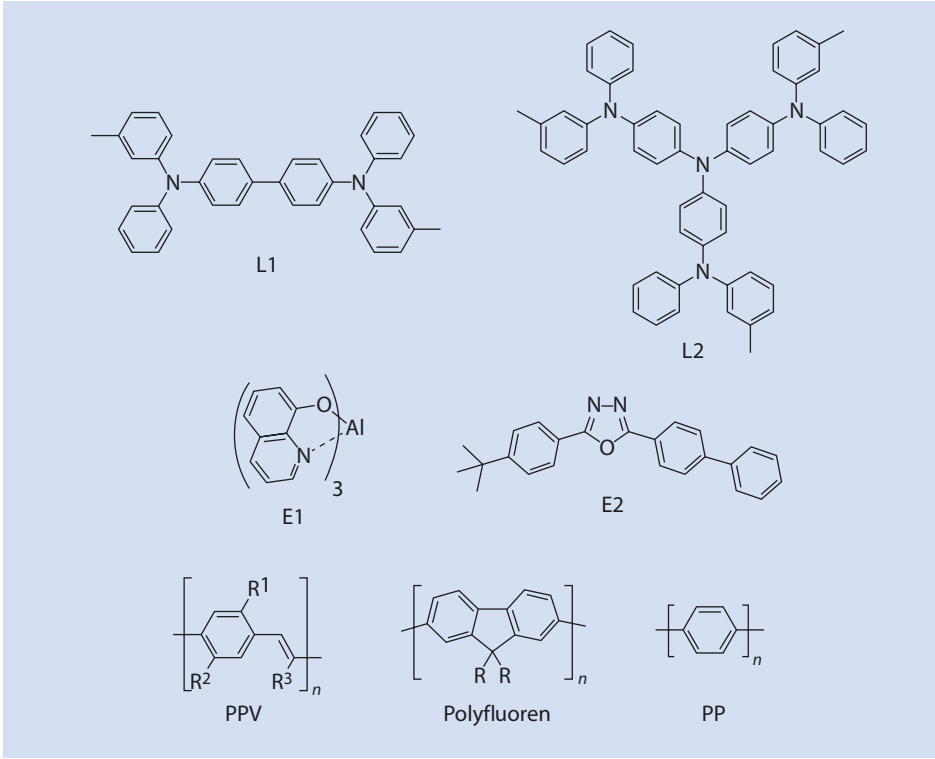

Fig. 22.11 Typical structures of monomeric hole and electron conductors and multifunctional polymers which can also function as emitters. *L1*, *L2* Hole conductors, *E1*, *E2* Electron conductors *PPV* *Polyfluorene*, *PP* Polymers

photo-cross-linking each layer as it is applied, thereby rendering it insoluble and preventing damage by the application of further solution layers. This procedure is illustrated in Fig. 22.12.

A polymer or a small molecule building block with at least two photochemically linkable side groups per molecule (e.g., oxetane groups) is applied onto a glass carrier with an ITO surface. After removing the solvent, the layer is cross-linked via the oxetane groups in the presence of a photoinitiator (▶ Chap. 10, Fig. 10.17) with the aid of UV light. Thereafter, the cycle can be repeated with a second and third polymer solution to produce a multilayer diode. A cathode is then applied and the whole construction is "encapsulated" and thus protected by a transparent, inert polymer layer.

Aromatic polyamines have proved successful as hole conductors as have oxetanes as cross-linking moieties. The basic structure of this type of system is shown in Fig. 22.13.

Both small molecule and polymeric aromatic amines can be elegantly synthesized by a Hartwig–Buchwald coupling (Louie and Hartwig 1995; Guram et al. 1995).

The required functional (electroluminescence and cross-linking) groups can also be incorporated into the polymer chain by copolymerization. The synthesis route, shown in Fig. 22.14, undoubtedly increases the possibilities for variation in the structure of

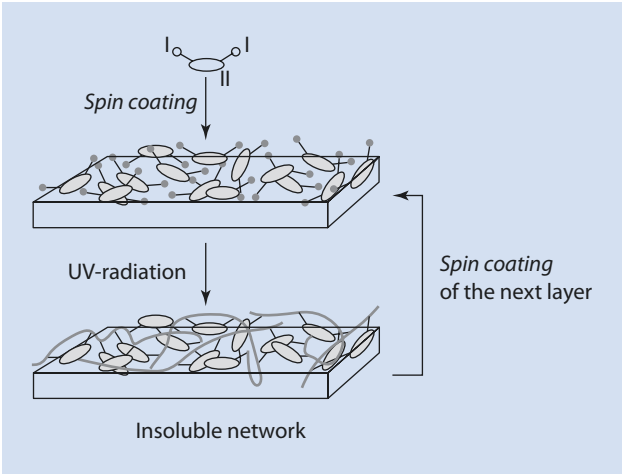

Fig. 22.12 Manufacture of a multi-layer OLED. *I* Cross-linkable group, *II* Electroluminescent monomer or polymer

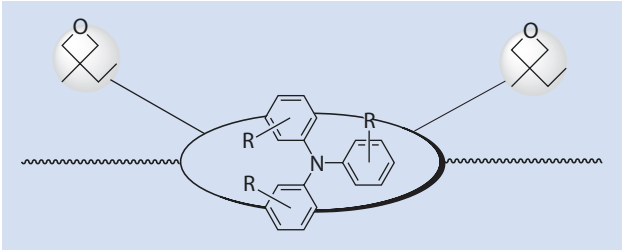

Fig. 22.13 Basic structure of an aromatic amine with cross-linkable side groups

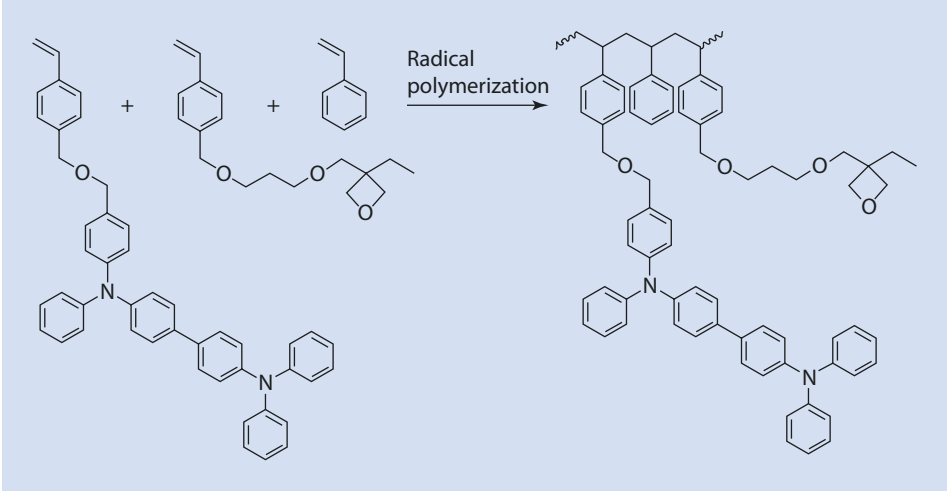

Fig. 22.14 Cross-linkable OLED-polymer via copolymerization

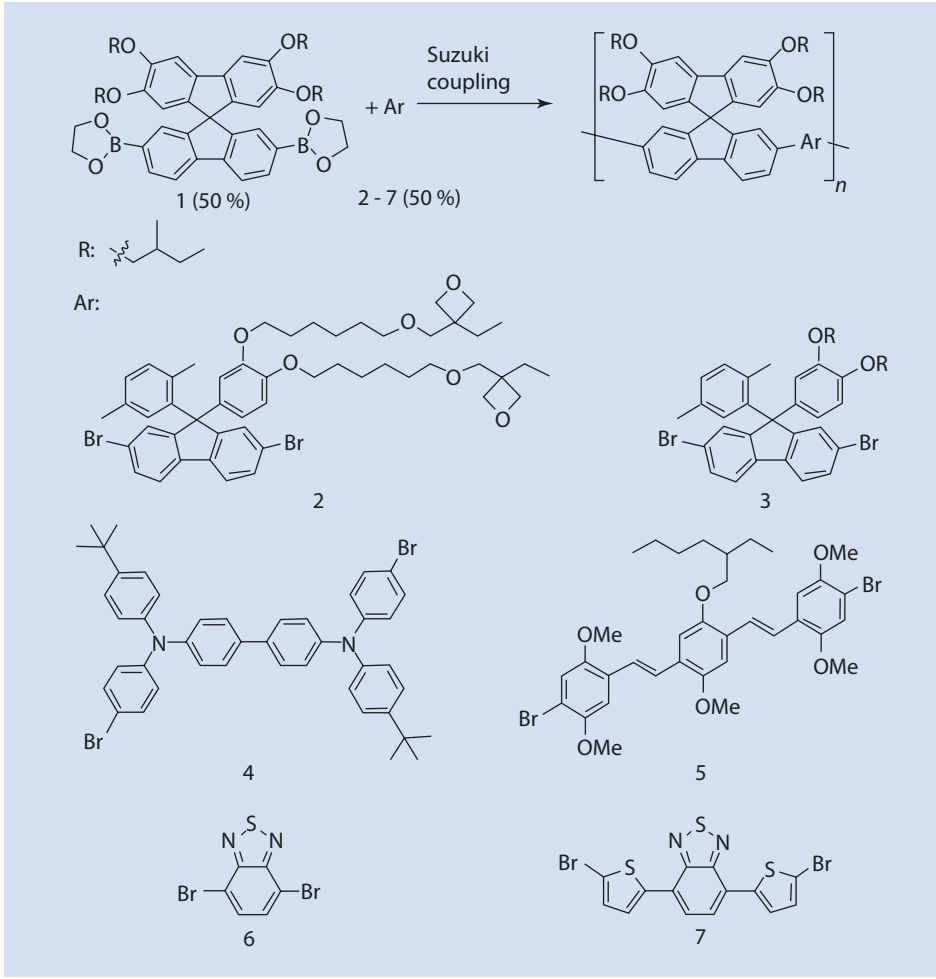

Fig. 22.15 Synthesis of blue, green, and red luminescent polymers by Suzuki-coupling

OLED materials. However, the backbone chain exhibits an undesired "dilution" of the functional groups.

Spin coating technology has been successfully used to make multicolor displays. The basic materials are produced by Suzuki coupling (Fig. 22.15) (Müller et al. 2003).

By combining different molar percentages of the building blocks **2**–**7** in relation to building block **1** (50 mol%), the three base colors blue, green, and red can be realized (Table 22.5).

If layers are irradiated through a mask, superfine colored structures remain, which can be addressed individually.

One important innovation is the Baytron®-initiated cross-linking of OLED polymers with oxetane side groups (Köhnen et al. 2009). Baytron® is a mixture of poly(3,4-ethylene dioxythiophene) (PEDOT) and polystyrene sulfonate (PPS). To produce a multilayer

Table 22.5 Proportions of the building blocks **1–7** from Fig. 22.15 in the OLED-polymers P-Blue, P-Green, and P-Red

Building block	P-blue	P-green	P-red
1	50	50	50
2	25	25	25
3	15	–	–
4	10	10	10
5	–	15	–
6	–	–	10
7	–	–	5

display, a PEDOT/PPS layer is covered with an oxetane-containing OLED polymer. Experience has shown that this layer can be "arbitrarily" thick. If the layer is heated to the glass transition temperature of the polymer to be cross-linked, it is completely cross-linked with the reaction starting at the interface with the PEDOT/PPS layer. Subsequently, a further cross-linkable layer of a different OLED polymer can be applied. By creating suitable conditions for cross-linking ($T > T_G$, t), this layer can also be cross-linked without any problem. Thus a multilayer display can be constructed very easily without the necessity of adding another (photo-) initiator.

The oxetane moiety in contact with PEDOT/PPS at the interface is apparently activated by a proton, initiating a cationic ring opening of the oxetane moieties and thus cross-linking, which propagates throughout the whole layer. This layer remains active on its surface, so its activity can be transferred to the subsequent layer. Again, complete cross-linking without the loss of activity is triggered, which can be transfer to the subsequent layer. Because of its size, PPS definitely cannot be considered as a counterion. An alternative is that, under curing conditions, PPS eliminates HSO_4-ions which accompany the active species on its journey through the layers.

Thus it comes as no surprise that OLED technology is said to have a bright future. In particular, it can be expected that large-surface, freely formable light sources and displays are possible using polymer building blocks. One challenge is to increase the efficiency and life expectancy of white light-emitting OLEDs. In addition, the hermetic encapsulation of displays remains another as yet unsolved challenge.

22.5 Polymer Membranes for Fuel Cells

Given the increasing scarcity of energy resources and the increasing environmental problems caused by traditional energy sources, it is not surprising that the field of fuel cells is attracting increased attention (Scherer 2008).

Fuel cells, electrochemical devices that directly transfer the chemical energy of fuel (hydrogen, methane, propane, methanol, etc.) into electricity using oxygen from the air

without resorting to a conventional combustion process have been known for a long time (Fig. 22.16).

The reduction and oxidation stages of the combustion reaction take place separately in the fuel cell. The two reactions take place in different parts of the fuel cell separated by an electrolyte membrane. Depending on the structure (Fig. 22.17 and Table 22.6), and especially on the electrolyte, positive or negative ions are transported through the membrane.

The fuel cell consists of a porous anode and a likewise porous cathode (e.g., of carbon fibers covered with activated carbon or carbon black doped with noble metals) which are separated by a membrane. High demands are placed on the membrane in terms of stability and efficiency.

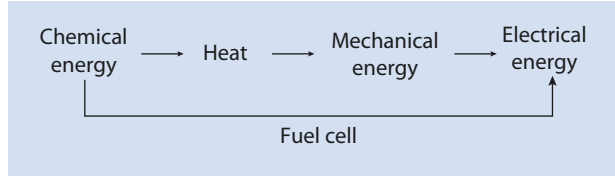

Fig. 22.16 Comparison of conventional conversion of chemical in electrical energy with fuel cells

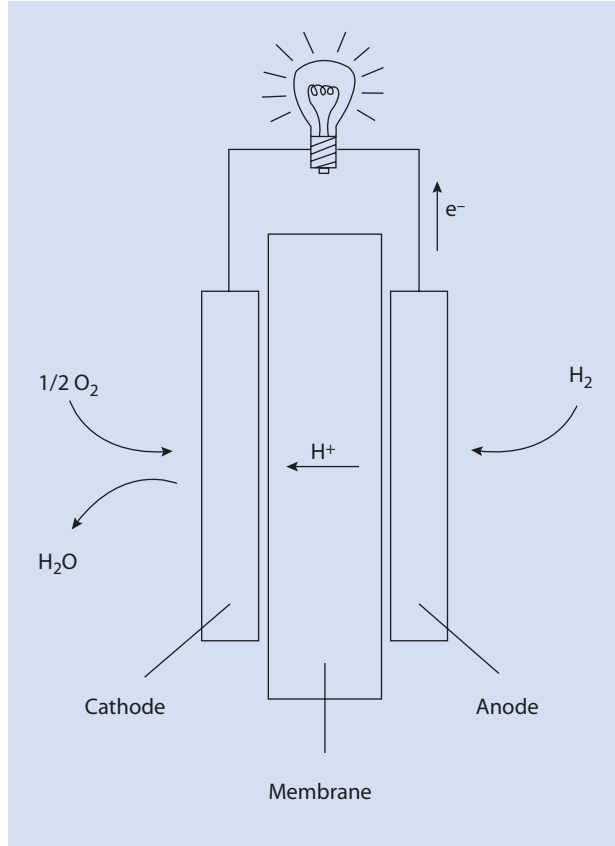

Fig. 22.17 Construction and mode of operation of a fuel cell. In this example protons are transported through the electrolyte, in this case the polyelectrolyte membrane

Table 22.6 Fuel cell types

Type	Electrolyte	Working temperature	Charge carrier	Application
PEFC	Ion exchange membrane	80 °C	H^+	Automobile
AFC	KOH	60–120 °C	OH^-	Space travel
PAFC	Immobilized phosphoric acid	200 °C	H^+	Power stations
MCFC	Molten immobilized carbonate	650 °C	CO_3^{2-}	Power stations
SOFC	Ceramic	800–1000 °C	O^{2-}	Power stations

PEFC Polymer electrolyte fuel cell, *AFC* Alkaline fuel cell, *PAVC* Phosphoric acid fuel cell, *MCFC* Molten carbonate fuel cell, *SOFC* Solid oxide fuel cell

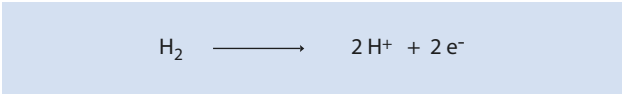

Fig. 22.18 Chemical reaction at the anode in a fuel cell

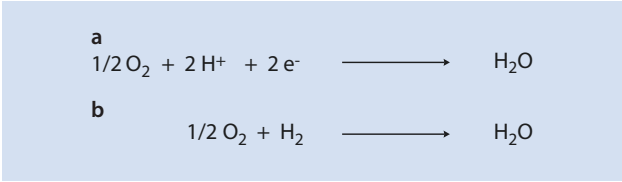

Fig. 22.19 (**a**) Chemical reaction at the cathode. (**b**) Complete fuel cell process

Hydrogen is separated into protons and electrons at the anode (Fig. 22.18). The electrons created on the anode can be used to produce electricity—they migrate to the cathode via an electrical circuit. The protons move through the polyelectrolyte membrane toward the cathode, driven by the electrical field. There the protons combine with oxygen and the electrons to form water (Fig. 22.19).

The following fuel cell types, depending on the type of membrane, can be distinguished (Table 22.6).

The membranes have special relevance. In the case of PEFC and PAFC, polymers are employed. Depending on the application, very different chemical structures have been suggested and indeed used. *Nafion*® (DuPont) with the structure shown in Fig. 22.20 is one of the most widely known polymer membrane materials.

Nafion® is a proton conductor whose conductivity can be attributed to the sulfonic acid groups in the side chains of the polymer but water is essential to the process. Because

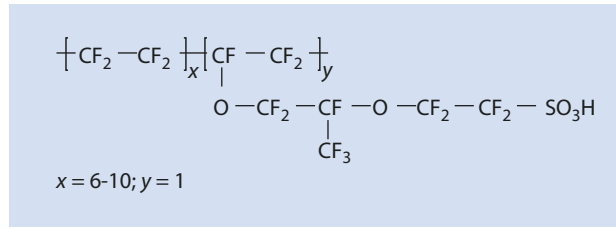

Fig. 22.20 Basic structure of Nafion®, a proton conductor

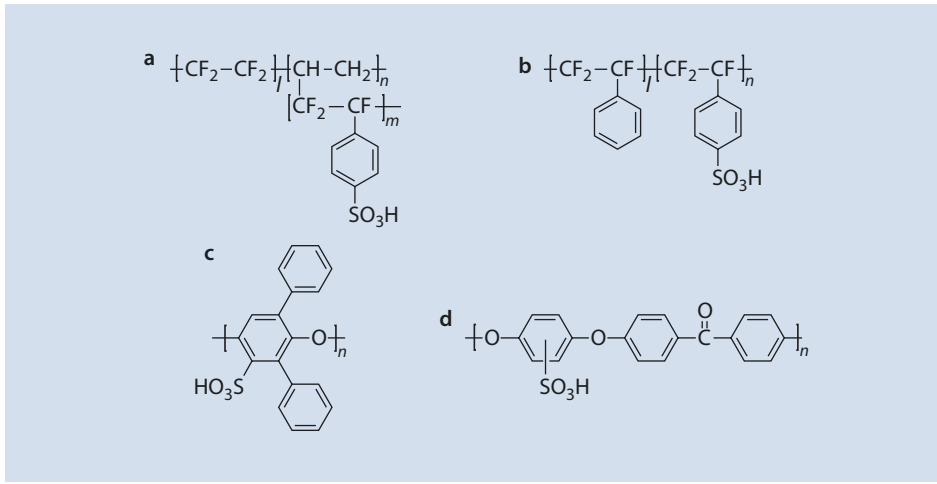

Fig. 22.21 Selected examples of proton conductors. (**a**) Scherer (1990). (**b**, **c**) Ballard Power Systems. (**d**) Maier and Meier-Haack (2008)

of the incompatibility of the sulfonic acid groups and the fluorinated polymer backbone, channels form in the polymer into which the sulfonic acid groups protrude. The transport of the protons occurs in these channels.

In Fig. 22.21, various alternative candidates for proton conductors are shown.

Ion transport depends heavily on water absorption. For example, Nafion® is an isolator in its dry state. Therefore, for most polymers, operating temperatures are not above 100 °C as loss of water by evaporation must be avoided.

Higher application temperatures can be reached with polybenzimidazole (PBI) doped with phosphoric acid (Fig. 22.22). Sulfonated PBI is also used as a proton transporter (Fig. 22.23).

Generally, the requirements of the membranes differ greatly depending on their application. For example, the use of PBI membranes in the car industry is problematic because of starting temperatures below 25 °C (the proton conductivity is too weak) and the formation of phosphoric acid when the car stops. However, for continuous use, for example, in power stations, these PBI membranes soaked in phosphoric acid, particularly because of their heat stability, provide an interesting solution.

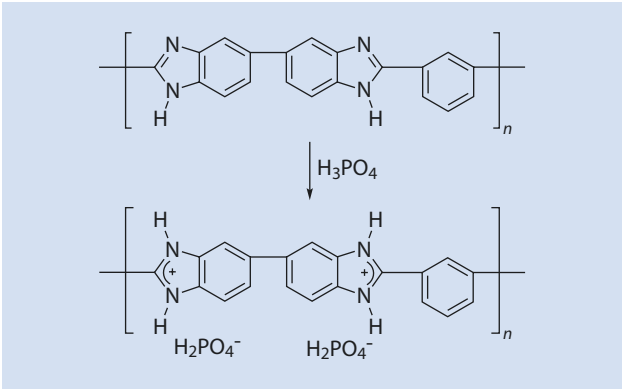

Fig. 22.22 Polybenzimidazole (PBI) -membrane modified with phosphoric acid (Samms et al. 1996)

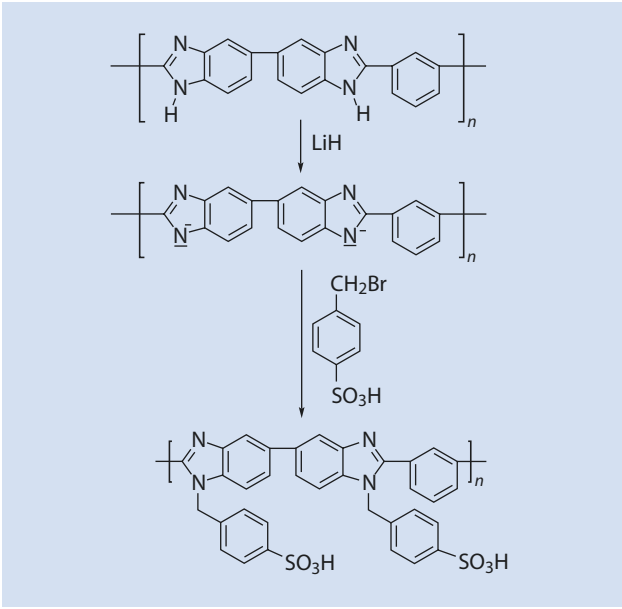

Fig. 22.23 Sulfonation of PBI (Glipa et al. 1997)

For future research, several major challenges remain to improve:

- Proton transport
- Mechanical stability, particularly the flexural fatigue strength necessary because of cyclic differences in the degree of swelling
- Thermal stability
- Chemical stability
- Permeability of reactants
- Cost efficiency

22.6 "Smart Polymers" in Oil Production

22

Originally, polymer science was mainly concerned with polymers as materials for making articles, such as films, fibers, adhesives, and other structural components. The spectrum was subsequently increased to include functional materials, such as super absorbers, conductive polymers, polymers for medicinal uses, and optics. When a polymer can fulfill different tasks under different circumstances, it can be called a "smart polymer." The concept of "smart polymers" is best explained by looking at an example, here their use in crude oil production.

When drilling for oil, not only oil fields but water veins are struck, resulting in about 3 tons of water being produced with each ton of oil. This results in 3 tons of waste or 40 billion dollars per year which must be used to extract and separation of the water. An intelligent solution would be to find a material that inhibits the water entering into the conveying shaft of the oil well but allows the oil to flow without restriction. Such a polymer might find and block the water (Shashkina et al. 2003). This material should exhibit a low viscosity as it is being injected, should gel when it comes into contact with water, but should retain its low-viscosity when in contact with oil (Fig. 22.24).

Polymers with a hydrophilic backbone and hydrophobic side chains are suitable for this task. They form physical gels in water (Fig. 22.25).

One example of such a polymer is a terpolymer of acrylamide, sodium acrylate, and an acrylamide, which is partially alkylated with a longer alkyl chain ($n = 8, 11$) and has a large molar mass ($M_w \approx 10^6$ g/mol) (Fig. 22.26).

If a watery solution of this polymer is pumped into the conveying shaft, the gel formation blocks both the water and oil transport. Only by adding an inhibitor that dissolves in water, but is insoluble in oil (e.g., a few wt% KCl) can the system be prohibited from gelling; the hydrophobic interactions are weakened and the chain is extended. If the carboxylate ions are converted to COOH, the hydrophobic interaction increases and a plug of gel closes the water supply. Thus, the intelligent solution works. The effect of the inhibitor is visualized in Fig. 22.27.

This "smart polymer" system serves to control the flow of water into the conveying shaft. It finds its own way to the water and blocks its influx by forming a gel.

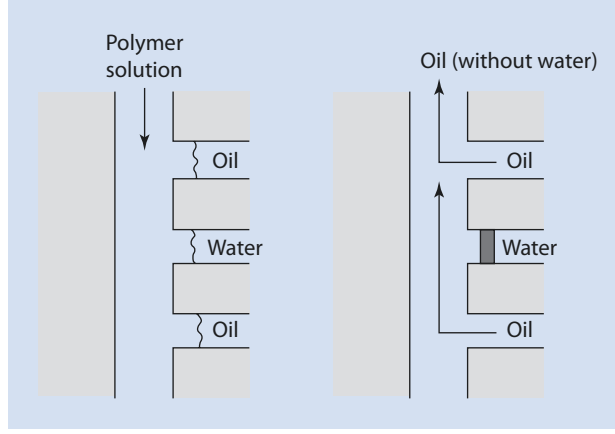

Fig. 22.24 Ideal behavior of a "smart polymer" during the production of crude oil

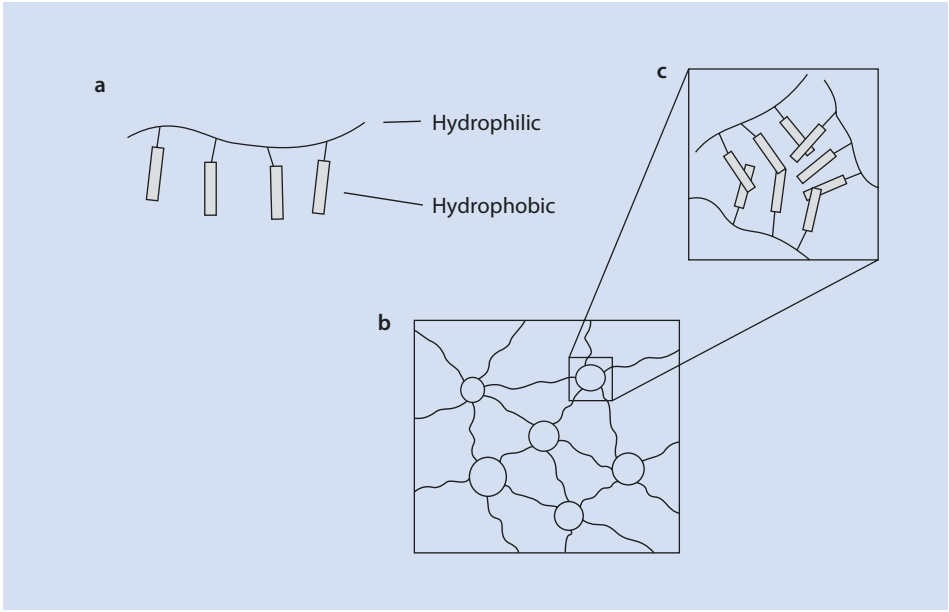

Fig. 22.25 (**a**) Schematic construction and (**b**) effect of a gelling polymer in water. (**c**) Detail showing a single cross-linked area

Fig. 22.26 Chemical composition of a "smart polymer" for the production of crude oil

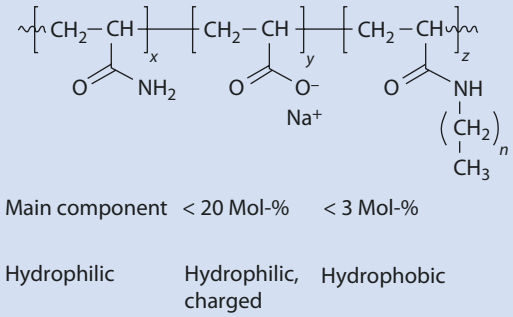

22.7 Graphene as Nanofiller

Until 2004, single-layered carbon coatings (graphene) were deemed thermodynamically unstable. The report on the preparation of graphene monolayers was for this reason all the more remarkable (Novoselov et al. 2004). For their work on graphene the main authors, A. Geim and K. Novoselev, were awarded the 2010 Nobel Prize for Physics.

If the single-layered carbon coatings are imagined in a convoluted form, then they form carbon nanotubes (CNT). If a portion of the six-membered carbon rings of the

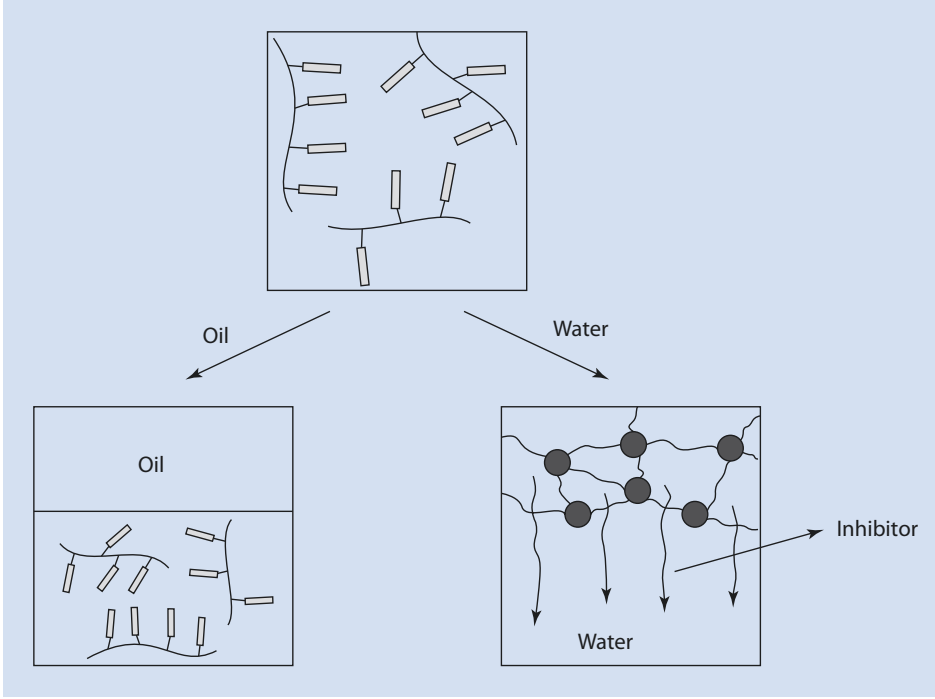

Fig. 22.27 Visualization of the effect of a "smart polymer" vis-a-vis water and oil

graphene are conceptually replaced by five-membered rings, the surface rolls into a sphere (fullerene).

The carbon atoms of the graphene are sp^2-hybridized, resulting in a two-dimensional honeycomb structure with C–C bonds of the same length (1.42 Å). The non-hybridized 2p-orbitals extend perpendicular to the graphene plane and form a delocalized π-bond system.

22.7.1 Graphene Production

The *exfoliation* of graphite—the mechanical separation of individual layers—was implemented by the aforementioned Nobel laureates. In this process, adhesive tape is pressed onto a graphite block and rapidly removed. The graphite monolayers—graphene—stuck to the adhesive tape are then transferred onto a wafer coated with photoresist as the adhesive tape is pressed onto the varnish and then removed. The graphene remains attached to the photoresist. After dissolving the photoresist, the graphene remains on the wafer.

An alternative route to producing graphene is a *top-down strategy*, which begins with graphite being oxidized to graphite oxide (GO). This is then neutralized with KOH, and then reduced (Fig. 22.28).

Alternatively, graphene structures can be synthesized following a *bottom-up strategy* with various preliminary stages. As an example, the synthesis of hexa-*peri*-hexabenzocoronene (HBC) is visualized in Fig. 22.29 (Clar and Ironside 1958).

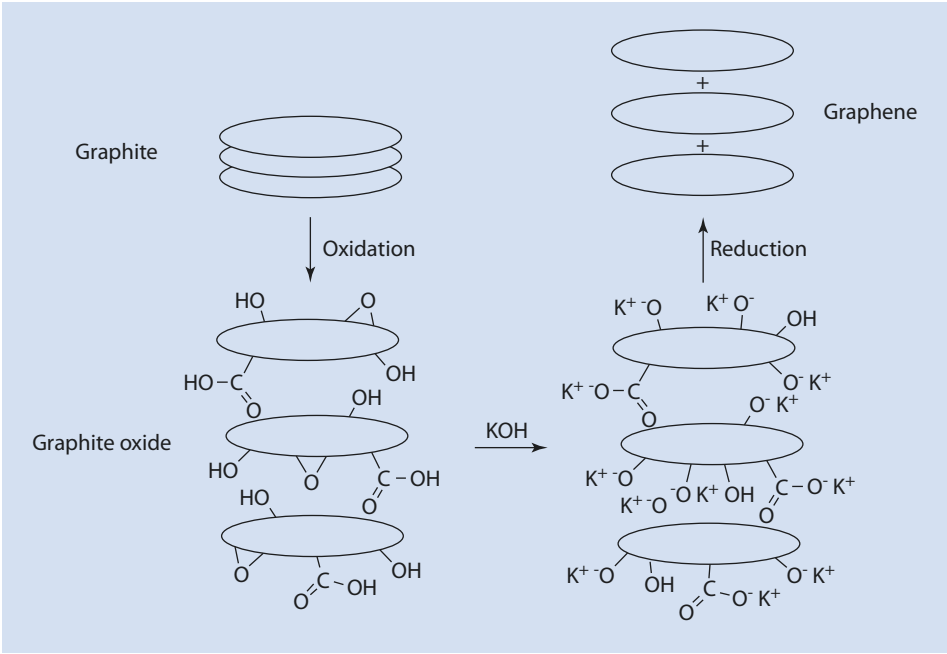

Fig. 22.28 Scheme showing the conversion of graphite to graphene via graphite oxide

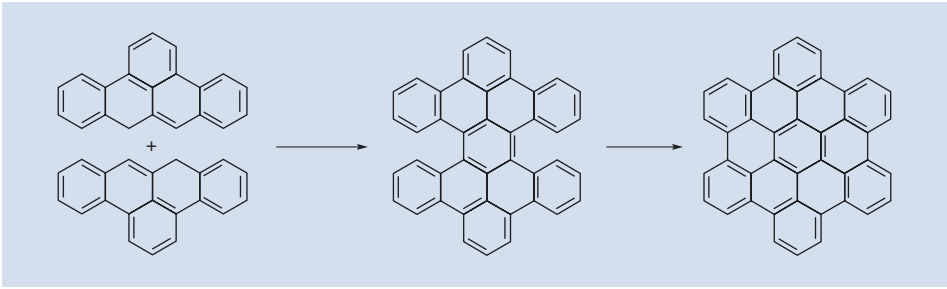

Fig. 22.29 Synthesis of hexa-*peri*-hexabenzocoronene (HBC), a precursor for graphene

The molecule presented in Fig. 22.30 is the largest polycyclic hydrocarbon known to date (Simpson et al. 2002). By modifying HBC it has been possible to produce a large number of well-defined, graphene-related molecules of various shapes and sizes (Wu et al. 2007).

Additionally, graphene can grow epitactically on metallic substituents, for example, by decomposition of ethylene on iridium. A further method for synthesizing individual graphene layers involves the thermal decomposition of hexagonal SiC layers. Graphene is a result of chemical vapor deposition (CVD) of carbon on inert substrates such as copper, which are subsequently dissolved.

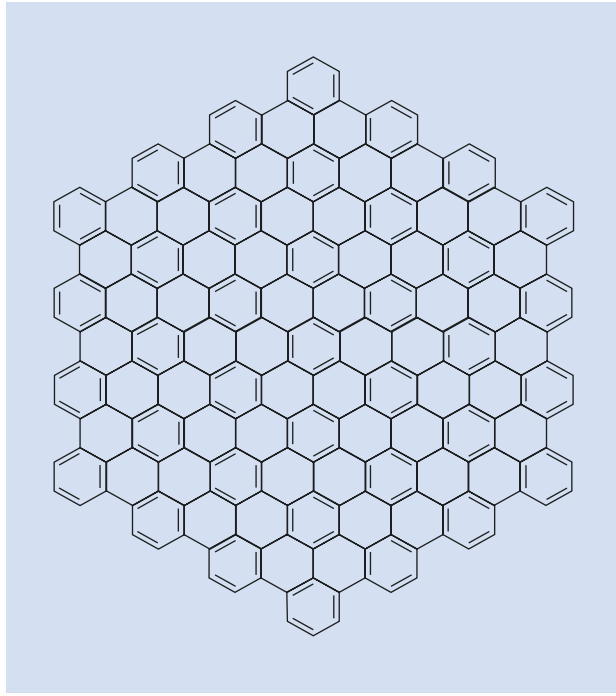

Fig. 22.30 Largest polycyclic hydrocarbon known to date

Table 22.7 Properties of selected fillers for polymers (Kuilla et al. 2010)

Material	Tensile strength (GPa)	Thermal conductivity (W m^{-1} K^{-1})	Electrical conductivity (S m^{-1})
Graphene	130	5000	7200
CNT	60–150	3500	4000
Steel	1770	5	135,000
HDPE	15	0.5	Isolator
Kevlar®	3600	0.04	Isolator

22.7.2 Properties and Use as a Nanofiller

Because graphene is two-dimensional, and consists of planar surfaces of sp^2-hybridized carbon atoms with a thickness of one atom, it is the thinnest material known to date.

Because of its unusual properties, such as high tensile strength and high thermal and electrical conductivity (Table 22.7), it is predestined as a filler for polymers suitable for use in "high-tech" processes such as in the field of electronic sensors, for flexible, transparent electrodes in displays, and in solar cells.

Polymer/graphene nanocomposites display excellent mechanical, thermal, and electrical properties when compared to their unfilled matrix polymers. For example, they have exceptional gas-barrier properties and flame resistance.

The thermal stability of a polymer can be improved by to 100 °C by filling it with graphene and even a small percentage of added graphene renders the composite electrically conductive. However, achieving an adequate dispersion of the strongly associated graphene particles is not trivial.

References

Cai Z (2006) Herstellung von Polymeren und Partikeln in einem. Spinning disk reactor. Dissertation, TU München
Clar E, Ironside CT (1958) Hexabenzocoronene. Proc Chem Soc, p 150
Echte A (1993) Handbuch der Technischen Polymerchemie**.** VCH Wiley, Weinheim, S 355
Friend RH, Gymer RW, Holmes AB, Burroughes JH, Marks RN, Taliani C, Bradley DDC, Dos Santos DA, Brédas JL, Lögdlund M, Salaneck WR (1999) Electroluminescence in conjugated polymers. Nature 397:121–128
Glipa X, El Haddad M, Jones DJ, Roziére J (1997) Synthesis and characterisation of sulfonated polybenzimidazole, a highly conducting proton exchange polymer. Solid State Ionics 97:323–331
Grund S, Kempe P, Baumann G, Seifert A, Spange S (2007) Zwillingspolymerisation: ein Weg zur Synthese von Nanokompositen. Angew Chem 119:636–640
Guram AS, Rennels RA, Buchwald SL (1995) Eine einfache katalytische Methode zur Synthese von Arylaminen aus Arylbromiden. Angew Chem 107:1456–1459
Köhnen A, Riegel N, Kremer JHWM, Lademann H, Müller DC, Meerholz K (2009) The simple way to solution-processed multilayer OLEDs—layered blockcopolymer networks by living cationic polymerization. Adv Mater 21:879–884
Kuilla T, Bhadra S, Yao D, Kim NH, Bose S, Lee JH (2010) Recent advances in graphene based polymer composites. Prog Polym Sci 35:1350–1375
Li D, Xia Y (2004) Adv Mater 16:1151
Louie J, Hartwig JF (1995) Palladium catalyzed synthesis of aryl amines from aryl halides. Mechanistic studies lead to coupling in the absence of tin reagents. Tetrahedron Lett 36:3609–3612
Maier G, Meier-Haack J (2008) Sulfonated aromatic polymers for fuel cell membranes. Adv Polym Sci 216:1–62
Müller CD, Falcou A, Reckefuss N, Rojahn M, Wiederhirn V, Rudati P, Frohne H, Nuyken O, Becker H, Meerholz K (2003) Multi-colour organic light-emitting displays by solution processing. Nature 421:829–833
Novoselov KS, Geim AK, Movozov SV, Jiang D, Zhang Y, Dubonos SV, Grigorieva IV, Firsov AA (2004) Electric field effect in atomically thin carbon films. Science 306:666–669
Pask SD, Nuyken O, Cai Z (2012) The spinning disk reactor: an example of process intensification technology for polymers and particles. Polym Chem 3:2698–2707
Ramshaw C (1983) Higee distillation—an example of process intensification. Chem Eng 389:13–14
Reneker DH, Chun I (1996) Nanometre diameter fibres of polymers, produced by electrospinning. Adv Mater 16:216–223
Samms SR, Wasmus S, Savinell RF (1996) Thermal stability of proton conducting acid doped polybenzimidazole in simulated fuel cell enviroments. J Electrochem Soc 143:1225–1232
Scherer GG (1990) Polymer membranes for fuel cells. Ber Bunsenges Phys Chem 94:1008–1013
Scherer GG (ed) (2008) Fuel cells I/II. Adv Polym Sci 215:1–268 and 216:1–261
Shashkina YA, Zaroslov YD, Smirnov VA, Phillippova QE, Khokhlov AR, Pryakhina TA, Churochkina NA (2003) Hydrophobic aggregation in aqueous solutions of hydrophobically modified polyacrylamide in the vicinity of overlap concentration. Polymer 44:2289–2293
Simpson CD, Brand JD, Berresheim JD, Przybilla L, Räder HJ, Müllen K (2002) Synthesis of a giant 222 carbon graphite sheet. Chem Eur J 8:1424–1429
Spange S, Grund S (2009) Nanostructured organic–inorganic composites by twin-polymerisation of hybrid-monomers. Adv Mater 21:2111–2116
Tang CW, VanSlyke SA (1987) Organic electroluminescent diodes. Appl Phys Lett 51:913–915
Wu J, Pisula W, Müllen K (2007) Graphene as potential material for electronics. Chem Rev 107:718–747